Mixed-Phase Clouds: Simulation of Optical and Radiative Properties

T. B. Zhuravleva
Institute of Atmospheric Optics
Tomsk, Russia

A. G. Petrushin
Institute of Experimental Meteorology
Obninsk, Russia

Introduction

Generally, the radiative properties of ice-crystal and mixed-phase clouds are studied using a plane-parallel, horizontally homogeneous cloud model. However, this model neglects horizontal inhomogeneity, a characteristic of the real clouds arising due to stochastic cloud geometry. In many cases, this neglect leads to unsatisfactory treatment of solar radiative transfer in the cloudy atmosphere. The present work is aimed at studying the combined effects of the random cloud geometry and cloud phase composition on the albedo R, diffuse transmittance Q_s, and angular distribution of solar radiation transformed by the "broken mixed-phase clouds-underlying surface" system.

Optical Characteristics of Mixed-Phase Clouds

Microstructure. The microstructure of mixed-phase clouds is determined by the microstructure of liquid- and ice-phase water and aerosol fractions. At the first stage of problem solution, we will neglect the aerosol component and assume that the clouds (from the viewpoint of phase composition) are homogeneous in space (Borovikov et al. 1961). For the ice-phase fraction, we will use the microstructure model of an ice-crystal cloud composed of ice plates and columns (Petrushin 1998). For the liquid-phase fraction, we will use the data on particle sizes and concentration in regions with mixed phase (Handbook of Clouds and Cloudy Atmosphere 1989).

Theoretical foundations of calculation of optical characteristics of mixed-phase clouds. The characteristics of radiation scattered by **ice** cloud medium (scattering phase function $P_{ice}(\theta)/4\pi$, scattering, extinction, and absorption coefficients α_{ice}, β_{ice} and ε_{ice}, and single scattering albedo ω_{ice}) are related to the corresponding characteristics of each ice component of cloud via the coefficients g_{col} (columns) and g_{pl} (plates) as

$$P_{ice}(\theta)/4\pi = g_{col} \times P_{col}(\theta)/4\pi + g_{pl} \times P_{pl}(\theta)/4\pi,\ \ 1/\omega_{ice} = g_{col}/\omega_{col} + g_{pl}/\omega_{pl} \tag{1}$$

$$\alpha_{ice} = \alpha_{pl} + \alpha_{col},\ \beta_{ice} = \beta_{pl} + \beta_{col},\ \varepsilon_{ice} = \varepsilon_{pl} + \varepsilon_{col},$$

where $g_{col} = \alpha_{col} / (\alpha_{col} + \alpha_{pl})$, $g_{pl} = 1 - g_{col}$.

For determining of characteristics of radiation scattered by **mixed-phase** cloud medium, it is necessary to know the coefficients k_{water} and k_{ice} (Petrushin 2001):

$$k_{water} = \alpha_{water} / (\alpha_{water} + \alpha_{ice}),\ k_{ice} = 1 - k_{water}, \tag{2}$$

where the subscripts "*water*" and "*ice*" refer to liquid- and ice-phase fractions, respectively. Then, the optical characteristics of mixed cloud can be written as

$$P_{mix}(\theta)/4\pi = k_{water} \times P_{water}(\theta)/4\pi + g_{ice} \times P_{ice}(\theta)/4\pi,\ 1/\omega_{mix} = k_{water}/\omega_{water} + k_{ice}/\omega_{ice}, \tag{3}$$
$$\alpha_{mix} = \alpha_{water} + \alpha_{ice},\ \beta_{mix} = \beta_{water} + \beta_{ice},\ \varepsilon_{mix} = \varepsilon_{waterl} + \varepsilon_{ice}$$

Equations (1) to (3) can be used to determine the optical scattering characteristics of an elementary volume of ice or mixed-phase cloud medium.

Let us evaluate the coefficients k_{water} and k_{ice} in terms of the fractions of liquid (p_{water}) and ice (p_{ice}) water contents of mixed cloud, given as functions of mean cloud temperature by Sundqvist (1993):

$$p_{ice} = 1 - A_0 \times \left(1 - \exp\left(1 - \chi_T^2\right)\right),\ p_{ice} + p_{water} = 1, \tag{4}$$

where $A_0 = 1.058$, $\chi_T = (T - 232)/24.04$, and T is the temperature of cloud layer (°K): 232° < T < 273°K. For convenience, we introduce the variables t and q:

$$t = p_{ice}/p_{water},\ q = k_{ice}/k_{water}, \tag{5}$$

which, for the cloud particle size distribution functions used here, are related by

$$q \approx Bt,\ B = A \times r_2 \times \left(\frac{N_{pl}}{(N_{pl} + N_{col}) \times \sqrt{S_{pl}}} \times \frac{K_{pl}}{K_{water}} + \frac{N_{col}}{(N_{pl} + N_{col}) \times \sqrt{S_{col}}} \times \frac{K_{col}}{K_{water}} \right) \tag{6}$$

Here K_{pl}, K_{col} and K_{water} are mean scattering efficiency factors for plate and column ice crystals and water droplets, S_{col} and S_{pl} are the mean areas of geometric shadow, and N_{col} and N_{pl} are concentrations for columns and plates, respectively. The S_{col} and S_{pl} values depend on ice crystal sizes and crystal shape factor (in the case of chaotically oriented convex crystals, the area of geometrical shadow equals a quarter of the particle area). The mean-squared radius of water droplet r_2 is connected with modal radius r_{mod} by the formula ($r_2 = (\nu + 1) \times (\nu + 2) \times r_{mod}/\nu^2$, in which ν is the parameter in exponential of gamma drop size distribution. For possible values of dimensionless parameters of size distributions $A \approx 4.08$ (Petrushin 1998).

Thus, from Eqs. (5) to (6), it follows that

$$k_{ice} = \frac{B \times p_{ice}}{1 - p_{ice} + B \times p_{ice}} \tag{7}$$

Optical calculation results. The characteristics of scattering of optical radiation by *ice columns* and *plates* were calculated as described by Petrushin (1998), while those for the microstructure model of the *liquid-phase* fraction of this cloud were determined by the method developed using well-known Mie-Lorenz theory (van de Hulst 1961). As initial ice crystal and water drop sizes, we took modal radius of droplets $r_{mod} = 2$ μm, $\nu = 6$; modal diameter of ice plates $d_{mod} = 40$ μm ($S_{pl} = 1.12 \times 10^3$ μm^2); and mean length of ice columns $1_0 = 50$ μm ($S_{col} = 1.22 \times 10^3$ μm^2). The ratio of column- to plate –shaped crystal concentrations was assumed to be $N_{col}/N_{pl} \approx 3$ (Heymsfield and Platt 1984). The complex refractive indices for ice m_{ice} and water m_{water} were taken from Warren (1984) and Rusk and Dudley (1971), respectively.

Calculations of scattering efficiency factors K_{pl} and K_{col} (Table 1) indicate that, for infrared wavelengths considered here, the mean ratio $K_{pl}/K_{col} \approx 1.02$, which almost coincides with $K_{pl}/K_{col} \approx 1.03$ at $\lambda = 0.63$ μm. Therefore, we set $g_{col} \approx 0.53$.

To calculate optical characteristics of ***mixed-phase*** clouds from Eq. (3), we need to know K_{pl}/K_{water} and K_{col}/K_{water}. In the visible and ultraviolet spectral range, these ratios are close to one. For longer wavelengths, accurate calculations of scattering efficiency factors for columns and plates must be made using data on microstructure of mixed-phase cloud components. This is because K_{water} depends strongly on both wavelength and corresponding droplet size distribution, whereas K_{pl} and K_{col}, for plates and columns large compared with wavelength of incident radiation, depend weakly on plate and column sizes (Volkovitskii et al. 1984).

The dependence of the ice contents of mixed cloud p_{ice} and the coefficient k_{ice} on cloud temperature and k_{ice} via p_{ice} is presented in Figure 1. Figure 2 shows scattering phase functions of mixed-phase cloud for wavelengths $\lambda = 0.63$ μm (B = 0.367) and $\lambda = 2.60$ μm (for $\lambda = 2.60$ μm, $m_{water} = 1.232 - i \times 0.004$, $K_{water} = 2.83$, $\omega_{water} = 0.963$, and B = 0.249).

Table 1. Calculations of scattering efficiency factors K for four different wavelengths.

λ, μm	$\mathbf{m_{ice} = n - i \times \kappa}$	$\mathbf{K_{pl}}$	$\mathbf{K_{col}}$	$\mathbf{K_{pl}/K_{col}}$
0.63	1.310 -i ×1,04(-8)	2.09	2.03	1.03
2.60	1.202- i×1.01(-3)	2.07	1.87	1.10
3.08	1.325 - i×6.25(-1)	1.21	1.21	1.00
3.97	1.365 - i×9.16(-3)	1.52	1.60	0.95

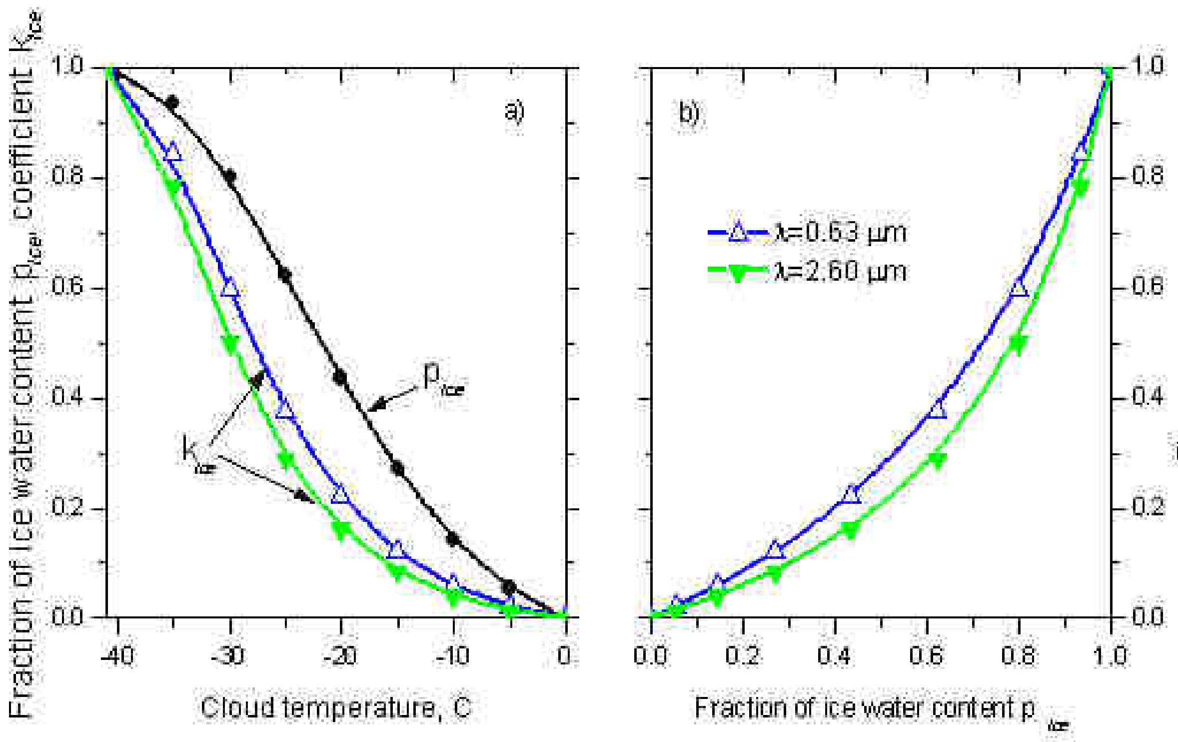

Figure 1. a) Influence of cloud temperature on fraction of cloud ice water p_{ice} and coefficient k_{ice}; b) dependence of the coefficient k_{ice} on fraction of cloud ice water p_{ice}.

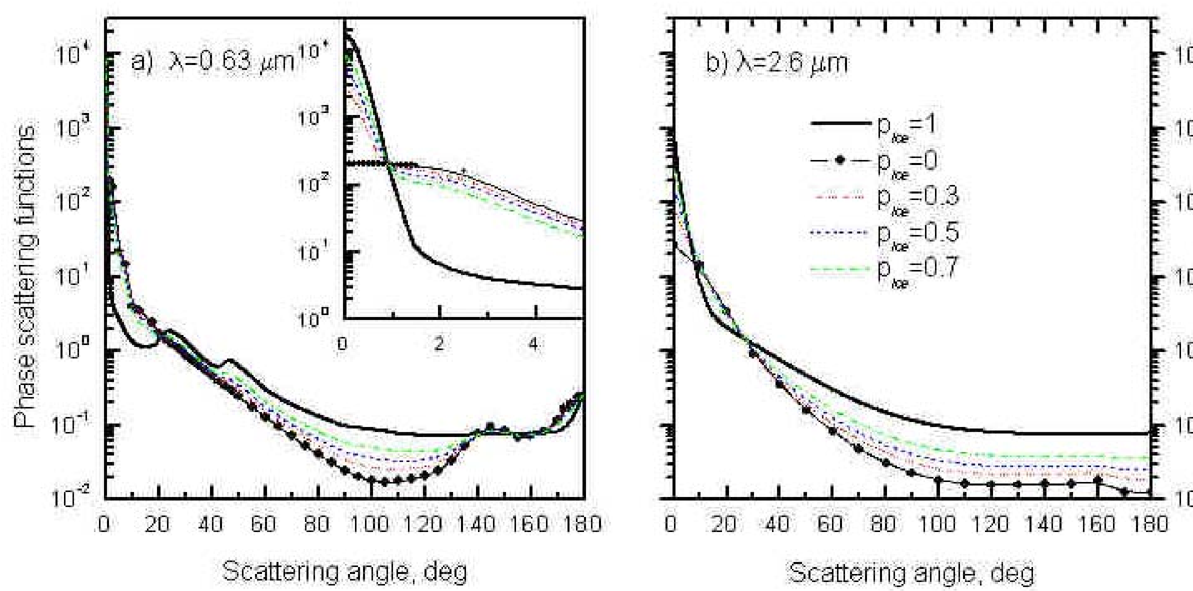

Figure 2. Dependence of cloud scattering phase functions on fraction of cloud ice water p_{ice}.

Radiative Effects of Mixed-Phase Clouds

Model and method of radiation calculation. The random nature of real broken clouds gives no way to uniquely describe the cloud-radiation interaction; therefore, we will use the **statistical description** of radiative transfer in clouds. The model of the cloudy-aerosol atmosphere and the Monte Carlo algorithm for calculating mean upward and downward fluxes of solar radiation in the near-infrared spectral range are given in (Titov and Zhuravleva 1997) in detail. It is assumed that a unit flux of solar radiation is incident on the top of the atmosphere H_{atm}^{top} in the direction $\vec{\omega}_{\oplus} = (\xi_{\oplus}, \varphi_{\oplus})$, where $\xi_{\oplus}$ and $\varphi_{\oplus}$ are solar zenith and azimuth angles. The underlying surface reflects according to Lambert's law.

We present computation results for mean albedo R, diffuse transmittance Q_s, and angular distributions of upward and downward solar radiances for mixed clouds. The mean angular distributions of upward (↑) and downward (↓) solar radiances will be characterized by the quantity

$$I^{\uparrow(\downarrow)}(z_*, \mu_i, \mu_{i+1}) = \left(\frac{1}{2\pi \times (\mu_{i+1} - \mu_i)} \times \int_{\mu_i}^{\mu_{i+1}} \int_{2\pi} \tilde{I}(z_*, \mu, \varphi) d\varphi d\mu \right),$$

where $\tilde{I}^{\uparrow(\downarrow)}(z, \mu, \varphi)$ is the mean scattered intensity in direction $\vec{\omega} = (\xi, \varphi)$ ($\mu = \cos\varphi$) at level $z = z_{\bullet}$. The integration limits (μ_i, μ_{i+1}) are chosen such that the difference between the corresponding zenith angles satisfies the relation $|\xi_i - \xi_{i+1}| = 5^{\circ}$.

Radiative calculation results. As is well known, the optical radiative transfer in the atmosphere is influenced substantially by such factors as stochastic cloud geometry and cloud phase composition, each important in its own right. How strong is their *combined influence* on fluxes and angular distributions of solar radiation?

To estimate the influence of **stochastic cloud geometry** on cloud radiative properties, we will compare calculations made for the horizontally homogeneous cloud model (PP clouds) with those for broken clouds (3D clouds). We consider a cloud field consisting of cloud bands with characteristic extents D_x and D_y along OX- and OY-axes, respectively. The bandwidth D_x (or D_y) is assumed to be comparable with cloud geometrical thickness H and much less than the band length D_y (or D_x). To estimate the influence of **phase composition**, we will calculate R, Q_s, and $I^{\downarrow(\uparrow)}$ for different fractions of cloud ice water in 3D and PP clouds.

We will quantify each of these factors in terms of the quantities

$$\Delta_{3D} F = 100\% \times (F_{3D} - F_{PP})/F_{3D}, \ \Delta_{ice} F = 100\% \times (F_{pice} - F_{pice=0})/F_{pice=0}, \ F = R, Q_s, I^{\downarrow(\uparrow)} .$$

The fluxes and angular distributions of solar radiation are calculated for cloud optical characteristics at $\lambda = 0.63$ μm. The radiative characteristics presented below are calculated for atmospheric levels $z_* = 0$ ($Q_s, I^{\downarrow}$) and $z_* = H_{atm}^{top}$ ($R, I^{\uparrow}$), solar zenith angle $\xi_{\oplus} = 60^{\circ}$, $\varphi_{\oplus} = 0^{\circ}$, surface albedo $A_s = 0.2$, cloud fraction N = 0.5.

Radiative fluxes. Calculations of albedo and diffuse scattered radiation for different cloud optical depths (Figure 3) show that

- The value of $\Delta_{3D}R\,(\Delta_{3D}Q_s)$ depends weakly on p_{ice} ($5 \le \tau \le 15$).
- As cloud optical depth τ grows, the influence of cloud random geometry on radiative fluxes considerably increases and reaches tens of a percent: for $0 \le p_{ice} \le 1$ and $\tau = 15$, $\Delta_{3D}R \approx 10 - 15\%$ and $\Delta_{3D}Q_s \approx 30\%$.

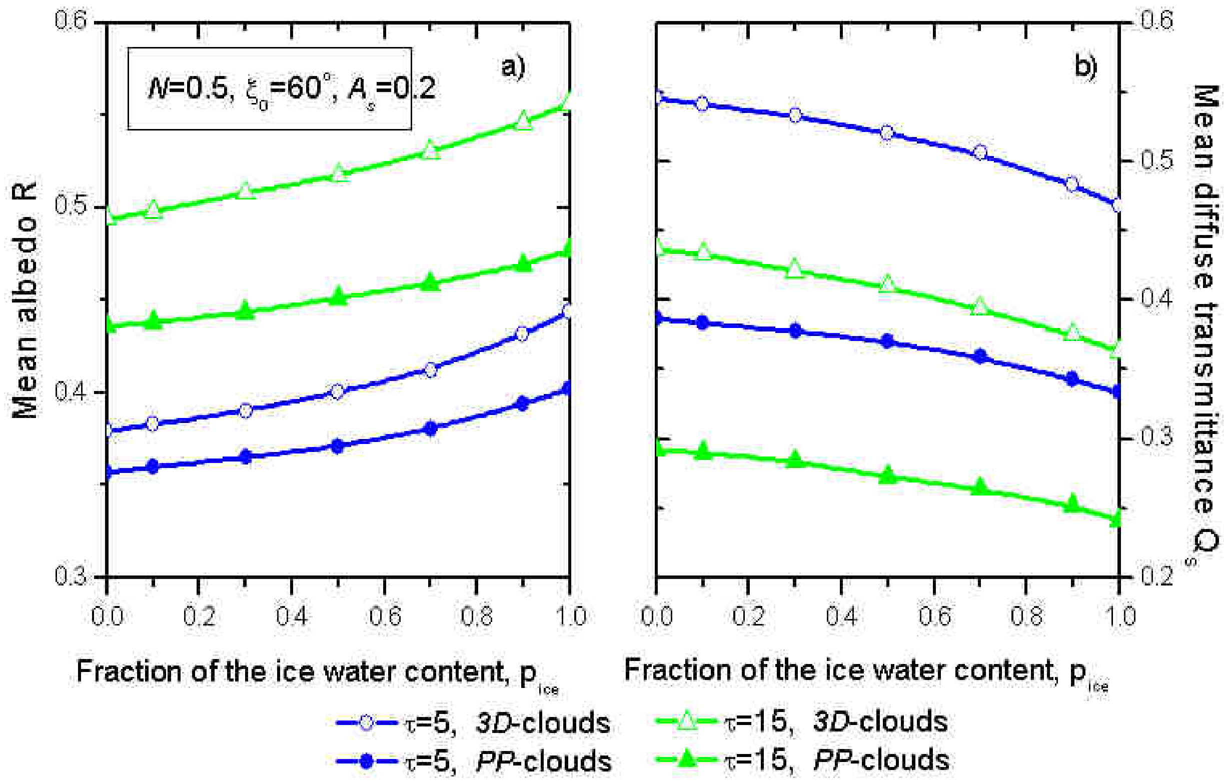

Figure 3. Fluxes of solar radiation as functions of the fraction of cloud ice water p_{ice} for different cloud optical depths with (3D) and without (PP) account of effects of cloud field random geometry.

The mean albedo of 3D clouds is a little more sensitive to phase composition than the albedo of PP clouds: e.g., at $\tau = 5$, and as p_{ice} increases from 0 to 1, $\Delta_{ice}R\,(3D) \approx 17\%$, whereas $\Delta_{ice}R\,(PP) \approx 13\%$. As cloud optical depth increases to $\tau = 15$, $\Delta_{ice}R$ decreases to ≈11% in 3D clouds and to ≈9% in PP clouds. The relative variations $\Delta_{ice}Q_s$ depend rather weakly on cloud field geometry (3D or PP clouds); they increase from $\approx -14\%$ to $\approx -17\%$ as the optical depth increases from $\tau = 5$ to $\tau = 15$.

Angular Distributions. The angular distributions of solar radiation are more sensitive (than fluxes) to geometrical structure of cloud field (Figure 4). Radiation passing through the cloud layer consisting of clouds of finite extents undergoes fewer scattering events than that transmitted by a horizontally homogeneous overcast cloud layer. Therefore, $I_{3D}^{\downarrow}$ is more sensitive to the scattering phase function than $I_{PP}^{\downarrow}$: for $\tau = 5$, $I_{3D}^{\downarrow} \approx 50\%$ (maximum biases $I_{3D}^{\downarrow}$ occur for viewing angles corresponding to "forward scattering" and 22° halo regions).

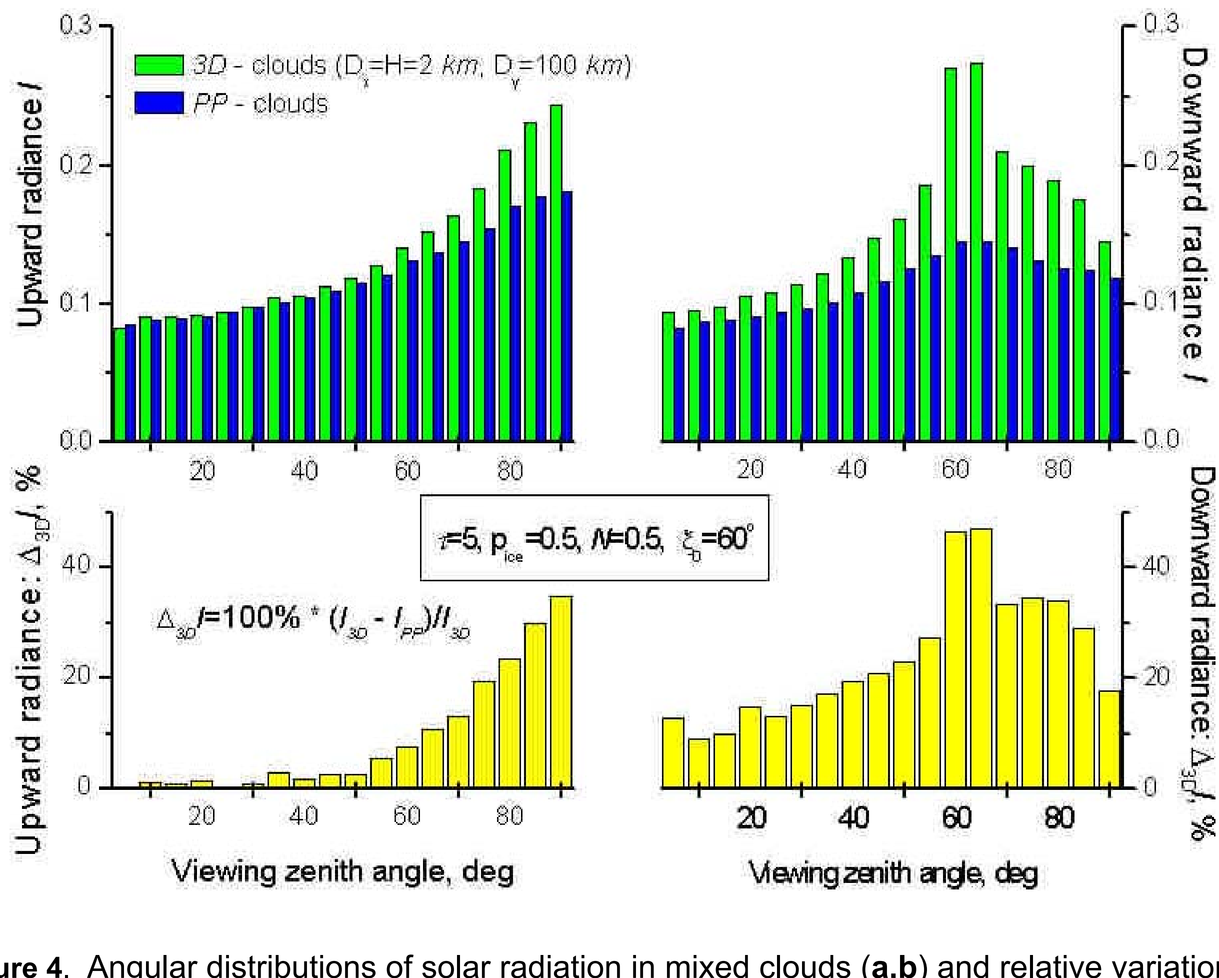

Figure 4. Angular distributions of solar radiation in mixed clouds (**a,b**) and relative variations of reflected and transmitted radiation $\Delta_{3D}I^{\downarrow(\uparrow)}$, caused by random cloud geometry (**c,d**).

Variations of the brightness field $\Delta_{ice} I^{\downarrow(\uparrow)}$, caused by the cloud phase changes, are presented in Figure 5. The increase of the ice water content (IWC) fraction in clouds leads to substantial change of angular structure. The maximum differences (>10%), both for 3D and PP clouds, are observed in the region of viewing zenith angles $\xi \leq 50^\circ$ for reflected radiation and in the angular region close to forward scattering direction $\xi \geq 40^\circ$ for transmitted radiation. The combined influence of phase composition and horizontal cloud inhomogeneity on $I^{\downarrow}$ is most significant for viewing angles $\xi \leq 30^\circ$.

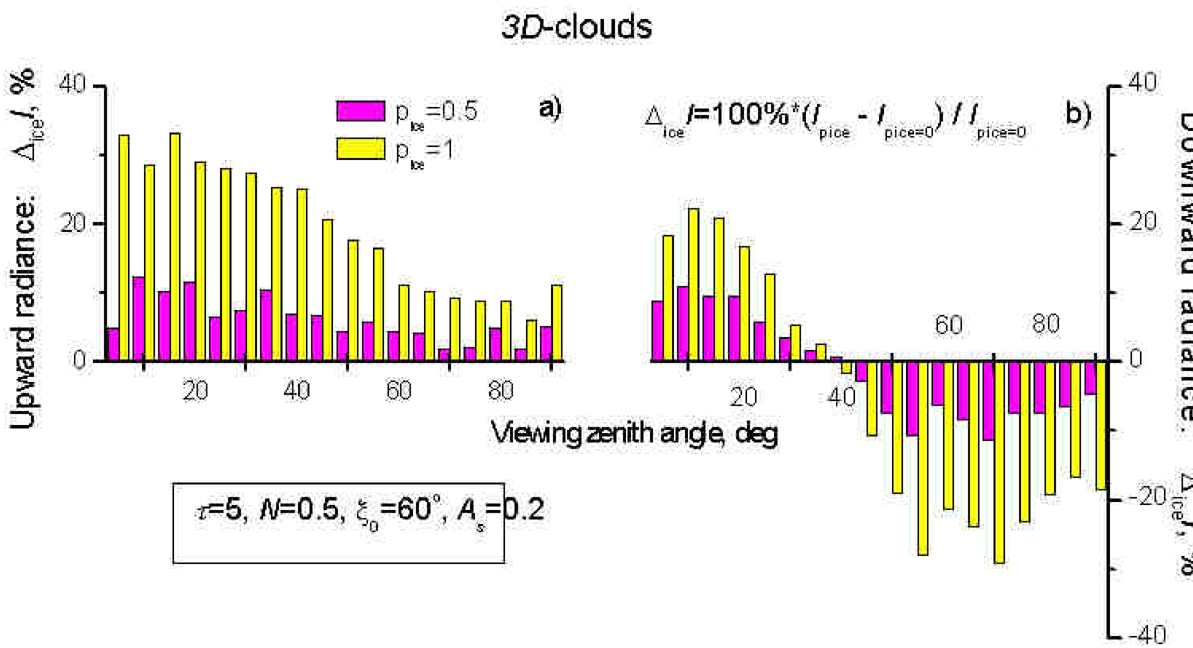

Figure 5. Relative variations of angular distributions of solar radiation $\Delta_{ice} I^{\downarrow(\uparrow)}$ caused by cloud phase composition.

The obtained results can be used to estimate, in the first approximation, how strongly the ***accuracy of determining IWC fraction*** in mixed clouds influences the accuracy of calculation of mean radiative fluxes. Let $p_{ice} = 0.5$ be the "true" value, and the relative error of p_{ice} determination is 100%; i.e., we misinterpret the mixed clouds as being either water or ice clouds. Then, for the cloud parameters indicated above, we must be aware of the fact (Figure 3) that the mean albedo will be either underestimated by ≈5% (if $p_{ice} = 0.0$ is assumed) or overestimated by ≈10% ($p_{ice} = 1.0$ for $5 \leq \tau \leq 15$).

An important factor that must be taken into account in interpretation of data of radiation measurements is the ***horizontal cloud inhomogeneity***. For instance, it is quite possible that the same mean albedo may correspond to clouds with different IWC fractions: e.g., for $\tau = 5$, $R(p_{ice} = 0.5, 3D) \approx R(p_{ice} = 1, PP)$ (Figure 3). The interpretation results can be improved, specifically using in analysis the data on downward fluxes of scattered radiation, since the Q_s variability caused by the horizontal inhomogeneity is more significant than the influence of cloud phase composition.

Future Work. In the near future, we plan to carefully study the fine structure of brightness fields of solar radiation, transformed by the broken ice-crystal and mixed-phase clouds in the visible and near-infrared spectral range. We also plan to estimate the errors in determining mixed-phase cloud properties arising due to lack of data on cloud phase composition (fraction of cloud ice water) over wide range of cloud optical parameters and observation conditions.

Acknowledgment

The work is supported partially by ARM contract "Cloud-Aerosol-Gas-Radiation Climatology in Central-Continental Stations" and Russian Fund for Basic Research (through the Grant 00-05-65456).

Corresponding Author

Tatiana B. Zhuravleva, ztb@iao.ru

References

Borovikov, A. M. et al., 1961: *Cloud Physics*. Gidrometeoizdat, p. 460, St.-Petersburg, Russia..

Handbook of Clouds and Cloudy Atmosphere, 1989. Eds., I. P. Mazin and A. Kh. Khrgian, Gidrometeoizdat, p. 648, St.-Petersburg, Russia.

Heymsfield, A. J., and G. M. R. Platt, 1984: A parameterization of the particle size spectrum of ice clouds in terms of the ambient temperature and the ice water content. *J. Atmos. Sci*., **41**, 846-855.

Petrushin, A. G., 1998: Optical radiation scattering and absorption in a crystalline cloud medium. *Problems of Clouds Physics*, Ed., L. P. Semenov, 118-149, Gidrometeoizdat, St.-Petersburg. (In Russian).

Petrushin, A.G., 2001: Main characteristics of scattering of optical radiation by mixed-phase clouds. *Izv. Akad. Nauk Rossii, Ser. Fiz. Atmos. Okeana* (in print).

Sundqvist, H., 1993: Inclusion of ice phase of hydrometeors in cloud parameterization for mesoscale and large-scale models. *Beitr. Phys. Atm*., N 66, 445-453.

Rusk, A. N., and W. Dudley, 1971: Optical constants of water in the infrared. *JOSA*, **61**, N 7, 895-903.

Warren, S. G., 1984: Optical constants of ice from ultraviolet to the microwave. *Appl. Opt*., **23**, 8, 1206-1225.

Titov, G. A., T. B. Zhuravleva, and V. E. Zuev, 1997: Mean radiation fluxes in the near-IR spectral range: Algorithms for calculation. *J. Geophys. Res.*, **102**, 1819-1832.

van de Hulst, 1961: Scattering of light by small particles. *Izd. Inostr. Literatury*, p. 536, Moscow.

Volkovitskii, O. A. et al., 1984: *Optical properties of ice clouds*. Gidrometeoizdat, p. 198, St.-Petersburg, Russia.